Proceedings of the ASME 2023 42nd International Conference on Ocean, Offshore and Arctic Engineering
OMAE2023
June 11-16, 2023, Melbourne, Australia

OMAE2023-104648

RELIABILITY ANALYSIS OF CRACK GROWTH OCCURRENCE FOR A SECONDARY STRUCTURAL COMPONENT DUE TO VIBRATION EXCITATION

Siri Kolle Kleivane
Norwegian University of Science and Technology
Trondheim, Norway

Bernt Johan Leira
Norwegian University of Science and Technology
Trondheim, Norway

Sverre Steen
Norwegian University of Science and Technology
Trondheim, Norway

ABSTRACT

Ship hull vibration is a significant contributor to fatigue crack growth and the major sources of vibrations are found to be the main engine vibration excitation, the wave-induced springing and whipping loads, and the action of the propeller. In the midship region, wave-induced loads and the main engine are the major contributors, whereas propeller excitation dominates in the aft region of the ship hull. The vibration problems onboard a ship are very complex and are found at both global and local levels. No general method exists to solve all kinds of vibration problems and hence they need to be evaluated through a cost-by-case approach. The complex and uncertain aspects of hull vibration and fatigue crack growth motivate the need for a reliability-based scheme for assessing the resulting fatigue crack propagation of secondary components and structural details. In the present paper, a probabilistic formulation for the failure probability of the occurrence of crack propagation of a secondary hull component is outlined. A generic cargo hold model is analyzed with engine excitation and wave-induced loading as vibration sources, and a stochastic model for vibration response is obtained based on this. The limit state is presented as the possible occurrence of crack growth. The secondary structural component considered is a pipe stack support, and different initial crack sizes are evaluated. The adequacy of the applied stochastic model for vibration response is evaluated and the accuracy of the estimated failure probability is assessed.

1. INTRODUCTION

Ship vibration continues to be a major concern in the design, construction, and operation of vessels. Excessive vibration may lead to the malfunction of machinery and equipment or fatigue failure of local structural members. The main engine, the propeller and the hydrodynamic loading are identified as the main sources of vibration. Vibrations are observed at both global and local levels and constitute a complex vibration picture within the ship hull. Hydrodynamic loading is considered to result in both local and global wave-induced vibration, generally described as springing and whipping [1][2]. Wave-induced vibration, along with main engine vibration, is dominant in the amidship region, while the propeller excitation is predominantly located in the aft end of the vessel, especially in the hull area above the propellers. The focus of this work will be on vibration caused by engine excitation and wave-induced loading.

Springing and whipping result in nonlinear vertical bending moments acting along the ship hull girder. This loading can be simplified as the superposition of high-frequency and low-frequency load components, which due to the interaction between various frequencies and components gives rise to coupled damage effects [3][4]. The vertical wave-induced bending moment results from the change of distribution of the buoyancy forces along the ship length combined with hydrodynamic and internal forces associated with the wave-induced ship motions [5]. For this loading condition on the ship hull, springing and/or whipping can occur. Springing is generally defined as stationary resonance vibration due to waves with encounter frequencies coinciding with the natural frequency, typically for the vertical 2-node mode [6]. Whipping is a transient hull girder vibration caused by an impact and is the vibration phenomenon which may follow after slamming and this transient vibration can increase the vertical bending moment [2][6].

The two-stroke low-speed marine diesel engines have been favored as the prime mover for ocean-going vessels due to their high reliability and efficiency. However, these engines transfer their vibration directly onto the hull structure, because the engine

is usually mounted directly onto the hull due to its large size and mass. The engine vibrations are generally categorized into external inertia forces and moments, resulting from the oscillating masses, and guide force couples, originating from the combustion process in the engine. The inertia moments have the potential to cause the largest vibration excitation in the ship hull and mitigation devices, such as moment compensators, are therefore most often installed to counteract the critical orders of these external moments. The guide force couples are usually harmless unless resonance conditions occur, and usually, no mitigation measures are taken for these types of vibrations. The guide force couples consist of so-called H-moments, which cause rocking of the engine, and X-moments which cause twisting of the engine.

The main objective of this work is not focused on the advanced modelling of the vibration sources, such as developing a model of the whole ship structure including the engine, but rather on the consequences of vibration with regards to fatigue crack growth of a secondary detail attached to the hull structure. In addition to the complexity of assessing ship hull vibration, fatigue crack growth is a very complex and uncertain phenomenon. Several parameters which describe the physics of the problem need to be considered and these are generally known only on an approximate level. Secondary structural components and equipment, such as supports for pipes and stringers, may be especially prone to crack growth if they are welded. Welded components are particularly susceptible to fatigue failure due to the welding procedure and the presence of the weld itself. The combined aspects of hull vibration and resulting fatigue crack growth motivate the need for a reliability-based scheme for assessing ship hull vibration and fatigue crack propagation of secondary details.

Previous research on reliability with regards to vibration and fatigue crack growth has largely focused on only one of the major vibration sources and typically either considered it on a global scale or a local scale. Much research investigates the prediction of and the consequences of vertical wave-induced bending moment, and springing and whipping, on the ship hull girder reliability, such as presented by [2], [5], [7] and [8]. Extensive investigations concerning fatigue crack growth of ships and offshore structures have been and continue to be made. Moreover, an increasing number of studies also investigate the probabilistic and reliability aspects of fatigue crack growth occurrence, such as presented by [3], [4], [9] and [10]. However, there is a limited amount of research which looks at vibration response by combining several major vibration sources and investigating the interaction of global and local vibration and its effect on secondary hull components or equipment. Such investigations are presented in this work to help improve the fatigue capacity of secondary details by the application of proper counteracting design measures.

2. CARGO HOLD FINITE ELEMENT MODEL AND VIBRATION ANALYSIS

A generic cargo hold finite element model has been developed consisting of ½ + 1 + ½ cargo hold units, divided by longitudinal bulkheads into transverse compartments as seen in Figure 1. Different filling levels (full, partially loaded, and empty) are modelled, and an alternating load condition is implemented. This is assumed as a scenario where the wall to which the pipe stack support is connected experiences large forces due to the mass of the cargo and the applied loading. The number of elements and nodes for each filling level case is given in Table 1. Boundary conditions are applied based on the guideline by DNV [11] for finite element analysis. The boundary conditions in the cargo hold analysis consist of rigid links applied at the model ends and a point constraint to restrict unwanted rotation of the model (see Table 3 in DNV-CG-0127 for further specification).

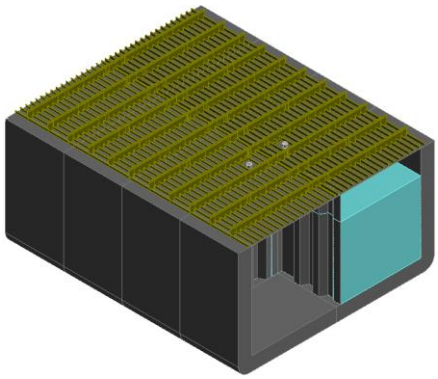

FIGURE 1: GENERIC CARGO HOLD MODEL, HERE SEEN WITH CARGO IN THE RIGHTMOST HOLD (75% FILLING LEVEL)

TABLE 1: FINITE ELEMENT MODEL NUMBER OF ELEMENTS AND NODES

Case	Elements	Nodes
Empty tanks	705740	1252199
25% filling level	729599	1331057
50% filling level	577286	1214706
75% filling level	732362	1330825
100% filling level	731348	1326467

The component under investigation is the pipe stack support, as seen in Figure 2. These components attach the cargo pump and its pipe stack to the tank wall. They are welded directly onto the tank wall during the installation of the pump at the shipyard. To investigate the vibration-induced stresses within the pipe stack supports, additional submodels are established and analyzed using the sub-modelling technique. The nodal displacements of the global model are applied to the corresponding boundary nodes on the local model and represent the boundary conditions for the submodel as prescribed displacements. This allows us to examine the behavior around a specific, locally refined area without affecting the overall stiffness of the model, which also implies that the computational time will be only a fraction of the time it would take to analyze the whole section model.

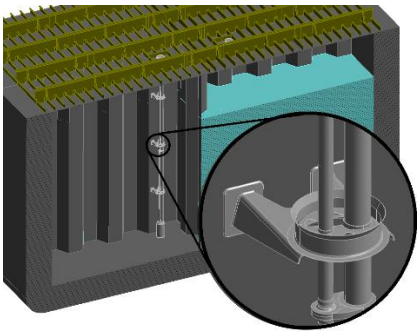

FIGURE 2: PIPE STACK SUPPORT CORRESPONDING TO THE SECONDARY STRUCTURAL COMPONENT UNDER CONSIDERATION

The vibration analyses are conducted using Ansys Workbench with the application of the loading due to the engine excitation and the vertical wave-induced bending moment. These loading conditions are simulated separately; the cargo hold model is analyzed for different combinations of engine rpm and filling level in one analysis case, and it is analyzed with different vertical bending moments implemented as loading in another case. The resulting stresses are the responses of interest since, in general, stress is considered to be the driving force for fatigue crack propagation. The type of stress evaluated is hot spot stress, which is obtained based on the recommended practice by DNV [12]. The modelling is based on solid elements also including the weld in the model. Based on this, the effective hot spot stress is taken as the stress read out from a point located 0.5*t* away from the weld toe in the region where the maximum stress occurs, and *t* is the plate thickness at this location. DNV then gives the following formula to calculate the effective hot spot stress:

$$\Delta\sigma_{HotSpot} = max\begin{cases} 1.12\sqrt{\Delta\sigma_{\perp}^2 + 0.81\Delta\tau_{\parallel}^2} \\ 1.12\alpha|\Delta\sigma_1| \\ 1.12\alpha|\Delta\sigma_2| \end{cases} \quad (1)$$

The factor α depends on the welding class of the detail (see Table A-3 in DNV-RP-C203), which for the current detail can be taken as C2 with manual fillet weld, giving a factor α of 0.90, and $\Delta\sigma_1$, $\Delta\sigma_2$ are the principal stresses calculated by:

$$\Delta\sigma_{1,2} = \frac{\Delta\sigma_{\perp}+\Delta\sigma_{\parallel}}{2} \pm \frac{1}{2}\sqrt{(\Delta\sigma_{\perp} - \Delta\sigma_{\parallel})^2 + 4\Delta\tau_{\parallel}^2} \quad (2)$$

3. PROBABILISTIC FORMULATION OF VIBRATION RESPONSE

Three stochastic variables are applied for the evaluation of vibration response: the engine speed in rpm, the percentage filling level of cargo in the tanks, and the vertical wave-induced bending moment. The engine speed is represented by the stochastic variable X with a corresponding probability density function (pdf) $f_X(x)$, the filling level is represented by the stochastic variable Y with a pdf $f_Y(y)$, and the vertical bending moment is represented by the stochastic variable Z with a pdf $f_Z(z)$. By assuming that the variables are statistically independent, then the resulting joint pdf can be expressed on the form:

$$f_S(x,y,z) = f_X(x) \cdot f_Y(y) \cdot f_Z(z) \quad (3)$$

The characteristics of the different stochastic variables are given in Table 2, and these will be further elaborated on in the following sections.

TABLE 2: CHARACTERISTICS OF STOCHASTIC VARIABLES

Stochastic variable	Engine speed (rpm)	Filling level (%)	Vertical moment (MNm)
Description	X	Y	Z
Distribution	Normal	Uniform	Weibull
Mean	86.1	50	-
Std	1.1	28.9	-
w	-	-	52.2
k	-	-	1
Upper – lower limits	80 – 90	0 – 100	1.5 – 105

* Std: standard deviation, *w*: scale parameter, *k*: shape parameter

3.1 Engine excitation

Modern engine manufacturing allows the manufacturer to analyze the engine performance already at the design stage, where excitation, structure and vibration response can be considered. Therefore, the engine manufacturer provides the data on external forces and moments from engine vibration of specific engines. The data in the current work is provided by the manufacturer for an engine typically used in medium-sized oil tankers, specifically a 6-cylinder MAN B&W G50ME-C9.5, at an engine rating of 6875 kW. From this data, 5 different rpms with their respective guide force couple moments are extracted and used in the vibration analysis for engine excitation. The specific guide force couple moments are given in Table 3.

TABLE 3: EXTERNAL GUIDE FORCE COUPLES MOMENTS

H-moment [kNm]			rpms		
Order	80	83	85	87	90
6	825.9	826.9	827.6	828.4	829.5
12	65.7	65.7	65.7	65.7	65.7
X-moment [kNm]			**rpms**		
Order	80	83	85	87	90
2	241.5	226.8	215.8	204.5	188.7
3	524.0	492.1	468.1	443.7	409.2
4	270.3	268.2	266.6	265.0	262.8
8	83.3	83.3	83.3	83.3	83.3
9	144.7	144.7	144.7	144.7	144.7
10	36.6	36.6	36.6	36.6	36.6

The operational speed of the engine will influence the forces and moments produced by the engine. This is because these external forces and moments are influenced by the oscillating masses and the gas excitation processes in the engine, which change for different engine speeds. The engine speed as a stochastic variable is assumed to be normally distributed. This is based on research by [13], where a dataset of 16 crude oil tankers was investigated for estimation of the fuel consumption-speed curve for ships. Moreover, the ship's speed in knots can be expected to be roughly linear with the shaft rpm [14]. By considering the speed interval for when the ship is sailing in the laden condition in the open sea, the speed is approximately normally distributed. Based on the assumption of a linear relation, the mean and standard deviation of the engine rpm can be computed by well-established statistical formulas. The following distribution shown in Figure 3 is then obtained for the engine rpm, ranging from 80 rpm to 90 rpm with statistical parameters as given in Table 2.

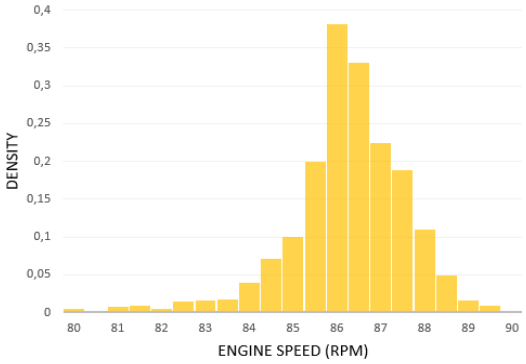

FIGURE 3: NORMALLY DISTRIBUTED ENGINE RPM, BASED ON DATA GIVEN IN [13]

The vibration analysis with engine speed excitation is done for combinations of five different rpms and five different filling levels in the tanks. The engine excitation is applied directly as moments scoped to a point mass which is a simplified representation of the engine, as seen in a) in Figure 4. The point mass is scoped to the aft end of the model as a remote point with connection lines as seen in b) in Figure 4. The magnitudes of the moments are established from the data provided by the engine manufacturer and implemented with their respective frequency of excitation.

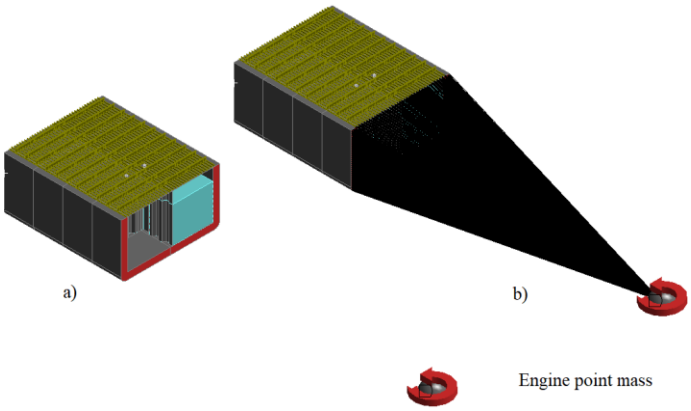

FIGURE 4: a) ENGINE EXCITATION APPLIED AS MOMENT, SCOPED TO POINT MASS, b) CONNECTION LINES OF REMOTE POINT DEFNINTION SCOPED TO AFT END OF THE MODEL

Five tank filling levels are applied in percentages which respectively correspond to the case of empty tanks, 25%, 50%, 75% and fully loaded tanks (100%). The filling level as a stochastic variable is assumed to be uniformly distributed, with characteristics as given in Table 2.

3.2 Vertical wave-induced bending moment

Typically, the long-term cumulative probability distribution function of maximum vertical wave-induced bending moment is well described by a two-parameter Weibull distribution, this was shown by [15] and [5], among others. The vertical wave-induced bending moment as a stochastic variable is assumed to be Weibull distribution with shape parameter k and scale parameters w as defined by [5] and based on the linear prediction of the IACS-CSR formulation [16]. The distribution parameters are given in Table 2. The nonlinear effect of the vertical bending moment is not taken into consideration at this stage.

Vibration analyses with a vertical moment applied as loading is performed for five different moment magnitudes, obtained by discretization of the assumed Weibull distribution. The maximum stress response at the support is obtained and based on this a functional representation of the stress due to vertical wave-induced bending moment is obtained. Since no consideration of nonlinear effects is made, thus assuming a linear bending moment, it may be expected (based on the load and the modelling simplifications) that there is a linear relationship between the stress response and the moment magnitude. For the full load, partial load, and ballast load conditions the Weibull equation remains the same and the loading imposed by the waves does not change. Hence, for simplicity, the vibration analysis of wave-induced loading is conducted with a constant filling level of 75% in the hold. However, it must be kept in mind that the response of the cargo hold model may vary with the filling levels of the tanks and further investigations of this may be necessary.

4. RELIABILITY METHODS AND LIMIT STATE FORMULATION

A large uncertainty is associated with fatigue crack growth and probabilistic methods are therefore commonly applied in the theoretical and numerical investigation of fatigue. Structural reliability assessments are applied to establish failure probabilities of structural systems at any stage during their service life. The reliability assessment of ships and offshore structures generally involves multiple limit states which are correlated, due to the complexity of such large systems. Therefore, simplifications are generally introduced to be able to analyze these systems. Simplifications are typically made in relation to the loading and response analysis, the strength characteristics and strength modelling, and how the different components and systems are connected. This introduces uncertainties in addition to the inherent uncertainties in the structural system.

The general reliability formulation (i.e., in terms of the probability of failure) can be expressed as:

$$p_f = P(G(\boldsymbol{x}) \leq 0) = \iint \dots \int_{G(\boldsymbol{x})\leq 0} f_{\boldsymbol{X}}(\boldsymbol{x}) d\boldsymbol{x} \qquad (4)$$

$G(\boldsymbol{x}) \leq 0$ is referred to as the limit state function and the failure probability is defined as p_f. The joint probability density function is defined as $f_{\boldsymbol{X}}(\boldsymbol{x})$, for the vector $\boldsymbol{x}$, which here is based on Eq. (3). Moreover, the expression in Eq. (4) cannot usually be solved analytically. Several different methods have been developed for solving this problem and extensively used are Monte Carlo simulation methods and FORM/SORM approximation methods.

The Monte Carlo simulation techniques generate a game of chance from known properties and involve simulating arbitrarily many experiments from random samples and observing the results to deduce the failure probability of the reliability problem. The original, most straightforward method may be called the crude Monte Carlo simulation or most often just Monte Carlo simulation. However, this method has a slow convergence of the estimated probability. To overcome this penalty, several different variance reduction techniques have been introduced creating a variety of different Monte Carlo simulation methods. A well-established method is the so-called importance sampling simulation. This method is based on applying identified information about the problem to constrain the simulation to the interesting regions, and fewer samples are needed to achieve the same level of accuracy as the original method.

The first-order reliability method (FORM) and second-order reliability method (SORM) are approximation methods which approximate the integral in Eq. (4) by transforming the problem from the given problem space, say *x*, to the standard normal space, say *u*. The methods then approximate the boundary of the area for which the event under investigation is fulfilled. The integration from Eq. (4) is then conducted over this area. The main difference between these two methods is that FORM approximates the event boundary using first-order surfaces, while the SORM uses second-order surfaces.

4.1 Limit state for fatigue crack growth

To illustrate the possible lifetime of a structural component, a simple event tree is presented in Figure 5. Assuming an initial crack is present in the structure there will either be crack growth or no crack growth. If there is no crack growth the component can generally be considered safe from fatigue failure. For inspection and maintenance, there are many different schemes and methods which can be employed, but generally, if an inspection is done it will either detect damage or not. Moreover, there are typically several inspections done during the lifetime of a component, and there may or may not be conducted repairs. However, for all cases, the eventual outcome is either that the component fails (F) or is safe (S) from fatigue failure, as seen in Figure 5. Note, even if repairs have been done the outcome may eventually still be a failure. In this work, we only look at the probability of the branch for the occurrence of crack propagation, but not looking further at the progression of crack growth.

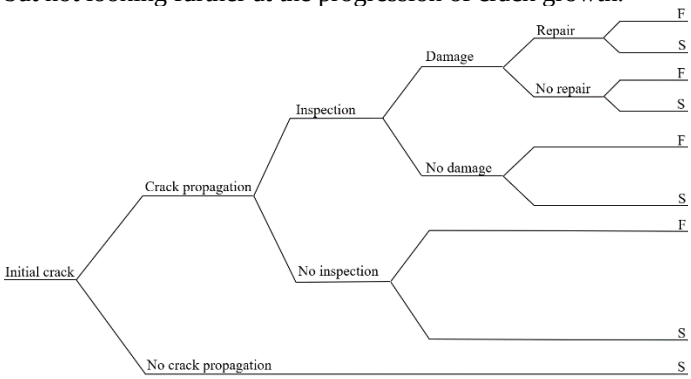

FIGURE 5: EVENT TREE FOR FATIGUE CRACK GROWTH, F: FATIGUE FAILURE, S: SAFE (NO FATIGUE FAILURE)

Reliability assessments are typically based on the likelihood of limit state violation. A limit state is considered to be a condition beyond which the structure or system does not fulfil its specified design criteria. The limit state formulation as defined in Eq. (4) gives the regions of the parameter space which correspond to safe or unsafe conditions. The limit state presently is formulated as the occurrence of crack propagation, assuming that a crack is already present in the pipe stack support. A typical assumption for a three-dimensional surface crack is a semi-elliptical shape. A fatigue stress limit may be defined below which there is no fatigue damage, meaning that a crack will not grow if the applied stresses are below this limit. This can be calculated based on an empirical expression for a stress intensity factor for fatigue crack growth [17], and the stress limit can be expressed as:

$$S_{limit} = \frac{\Delta K_{th}}{\sqrt{\pi \frac{a_i}{Q}} F} \qquad (5)$$

Where a_i is the initial crack size, F is a geometry factor, and ΔK_{th} is a threshold stress intensity factor for fatigue crack growth, values of which are typically found in the literature. The function Q is a shape function for an ellipse given as:

$$Q = 1 + 1.464\left(\frac{a}{c}\right)^{1.64} \quad (6)$$

where a is the crack depth and c is half the surface length for a crack with a semi-elliptical shape. The limit state function corresponding to the occurrence of a propagating fatigue crack is then formulated as:

$$G(x) = S_{limit} - g_S \leq 0 \quad (7)$$

where g_S is obtained based on the stresses resulting from a set of analysis cases corresponding to the random variables with joint pdf given by Eq. (3).

The initial crack size in welded structures is very difficult to establish and different research works presented in the literature provide different estimates (e.g., [18][19]). Moreover, the geometry function is dependent on the initial crack size, the crack geometry, and the configuration of the loading. To evaluate the effect of crack size on the geometry function and the fatigue limit, different initial crack sizes are investigated. Table 4 gives fatigue limits for different initial crack sizes using a recommended threshold stress intensity factor for steel of 63 MPa$\sqrt{\text{mm}}$ [18].

TABLE 4: FATIGUE LIMITS FOR DIFFERENT INITIAL CRACK SIZES

Analysis case	Initial size [mm] a_i	c_i	F [-]	S_{limit} [MPa]
1	0.1	0.3	1.0	125
2	0.2	0.5	1.0	91
3	0.3	0.5	1.0	82
4	0.4	0.8	1.0	68
5	0.5	1.0	1.0	60
6	0.6	1.0	0.95	61

Establishing an exact criterion for the acceptable probability of failure is challenging as it needs to be based on different aspects and parameters which generally only are known on an approximate level. This might be based on experimental investigation and operational experience. Moreover, for the investigations presented here, no such information is available but a probability of failure between 1 – 5 % is considered as not being critical for the pipe stack support. At this stage, any type of inspection and maintenance is not included in the model. The limit state formulation elaborated on here represents a conditional event of a propagating crack. This corresponds to the lifetime failure probability, and from this, the annual probability could then be computed as the probability increment per year as a function of time.

5. RESULTING RELIABILITY MODEL AND PROBABILITY ESTIMATION

5.1 Stochastic model of vibration response

The engine speed variable X is fitted by means of harmonic functions as shown in Figure 6, based on the response function given in Eq. (8).

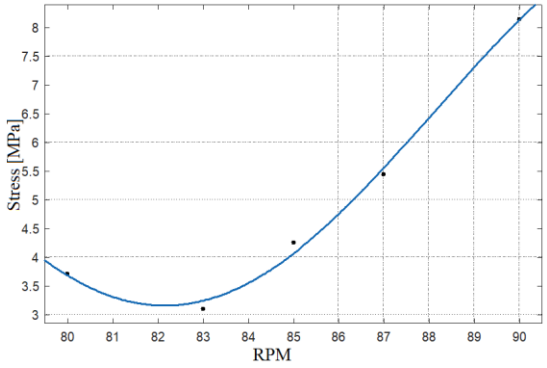

FIGURE 6: ENGINE SPEED RESPONSE CURVE

$$g_1(x) = 6.54 + 3.12\cos(0.26x) - 1.30\sin(0.26x) \quad (8)$$

The stress response corresponding to the filling level variable Y is fitted to a Gaussian equation as plotted in Figure 7, with the corresponding response function given in Eq. (9).

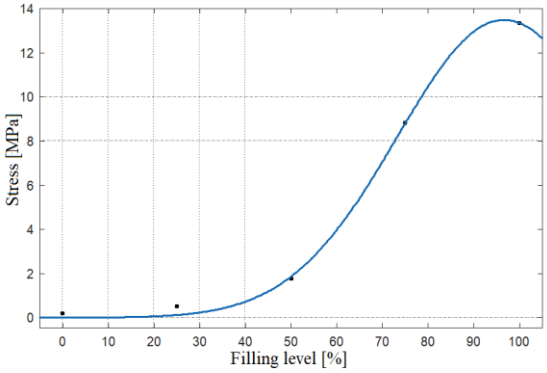

FIGURE 7: FILLING LEVEL RESPONSE CURVE

$$g_2(y) = 13.49 \cdot e^{-\left(\frac{y-96.61}{33.12}\right)^2} \quad (9)$$

The stress response due to the moment variable Z is fitted to a linear equation as plotted in Figure 8, with the corresponding response function given in Eq. (10).

The response functions in Eqs. (8), (9) and (10) give the vibration response due to each stochastic variable in form of stress with unit MPa.

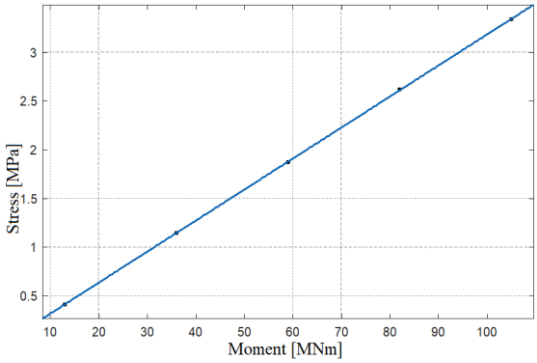

FIGURE 8: BENDING MOMENT RESPONSE CURVE

$$g_3(z) = 0.0318 \cdot z - 0.0027 \qquad (10)$$

The goodness of fit for the established response functions is evaluated based on three statistical parameters as given in Table 5. The sum of squares due to error (SSE) should have a value as close to zero as possible, the R-square should be as close to the value one as possible, and the root mean squared error (RMSE) should have a value as close to zero as possible.

TABLE 5: GOODNESS OF FIT STATISTICS

Variable	SSE [MPa^2]	R-square [-]	RMSE [MPa]
X	0.079	0.995	0.269
Y	0.193	0.999	0.312
Z	0	1	0.01

The goodness of fit for the Z variable is satisfactory, as can be assumed for a linear fit. For the X and Y variable, the SSE and R-square are satisfactory. This means there is only a minor deviation of the response values from the fit to the response values from the data, and the fit is successful in explaining the variation of the data. The RMSE, however, is sufficient but not optimal for X and Y.

The resulting stress response for a given combination of sample values of the random variables X, Y, and Z is obtained by the multiplication of the normalized versions of the two response functions $g_1(X)$ and $g_2(Y)$, and then summation with the normalized version of $g_3(Z)$. This is done as we have two analysis cases, the first case with engine excitation from which the response functions $g_1(X)$ and $g_2(Y)$ are obtained, and the second case with wave-induced loading from which the response function $g_3(Z)$ is obtained. The response functions are normalized to obtain the correct unit of stress (MPa).

An unsafe limit state condition is reached when the resulting stress from this combined response function exceeds the fatigue limit stress established by Eq. (5), as formulated in Eq. (7). The combined response function is based on the assumption of statistical independence. This is to some extent reasonable for the X and Y variables since the ship's speed is generally determined based on the voyage together with environmental conditions and is not related to the amount of cargo being transferred. However, the Z variable may be correlated to both the X and Y variables, since the magnitude of the moment is dependent on buoyancy forces, and hydrodynamic and internal forces associated with the wave-induced ship motions, for which all are dependent on the ship's speed and mass of the vessel (which is affected by the cargo).

The vibrational data set based on five different rpms and filling levels is a relatively small set of data. However, due to the computational demand for each simulation, a trade-off between simulation time and the number of data points simulated was necessary. Moreover, for the wave-induced vertical bending moment, nonlinear effects have not been considered. These simplifications represent limitations in the adequacy and accuracy of the developed stochastic model.

5.2 Failure probabilities

The estimated failure probabilities are presented in Table 6 for the different analysis cases given in Table 4. The Monte Carlo simulation is run with 500 000 samples and for the importance sampling simulation (DSPS) 100 000 samples were used. Proban is very fast in its calculations, and these sample sizes run in a matter of seconds and are deemed sufficient to obtain stable results in the probability calculations. The result from the Monte Carlo simulation and the importance sampling simulation coincides with those of the SORM approximation, while the FORM approximation deviates from the others. This may indicate that the failure surface is of second order or higher, displaying nonlinear characteristics. Therefore, the approximations by FORM may not be as accurate as the other estimates. The similarity in failure probability estimation from MC, DSPS and SORM methods provided support for the integrity of the obtained values. However, these results have not been compared with experimental or measured data. The accuracy of the results is only compared between the applied numerical methods, which must be kept in mind when discussing the credibility of the estimated failure probabilities.

TABLE 6: ESTIMATED FAILURE PROBABILITIES

Analysis case	Failure probability [%] MC	DSPS	FORM	SORM
1	-	0	0	0
2	$0.8 \cdot 10^{-3}$	0.001	0.002	$0.8 \cdot 10^{-3}$
3	0.026	0.025	0.054	0.022
4	0.837	0.824	1.596	0.746
5	3.207	3.227	5.472	3.099
6	2.777	2.759	4.812	2.640

*MC: Monte Carlo simulation
*DSPS: Design point simulation (importance sampling)

For increasing initial crack sizes, the probability of failure increases, which is as expected. Evaluating the failure probabilities in relation to the specified criterion for acceptable probability, the combined loading of engine excitation and wave-induced loading implies that the occurrence of crack growth is not likely. However, it cannot be concluded that the pipe stack support will not experience crack growth. This is one of the

drawbacks of probability assessments; the acceptance criteria are very difficult to establish. To have acceptable accurate target values they need to be based on both accurate descriptions of loads and responses, previous experience, and assessments of the consequences of fatigue failure. Therefore, based on the available information and provided data in this work, it can only be concluded that the evaluated problem has failure probabilities that are not critical concerning the occurrence of crack propagation.

The occurrence of crack growth has only been evaluated for a random point in time. A next step for further development of the framework herein may then be to evaluate loading over time until crack growth occurs (if this occurs, although with a relatively low probability) and investigate the time it takes for an initial crack to grow to a critical size which can be considered as representing fatigue failure of the component.

6. CONCLUSION

The functional representations of the stochastic variables are sufficiently satisfactory regarding the evaluation of their statistical parameters. The estimated failure probabilities imply that crack propagation is quite unlikely to occur. However, the component cannot be concluded as being completely safe with regards to the occurrence of crack growth, it can only be concluded that the evaluated problem is not a critical issue. The next step for further investigations may then be to evaluate loading over time for the branch of the event tree which represents the occurrence of crack growth and then evaluate the probability that a propagating crack will reach a critical level. It is believed that further development of the reliability model for the support component presented herein may help to establish a framework and a computational tool to improve the fatigue capacity of such components.

REFERENCES

[1] Storhaug, G., The measured contribution of whipping and springing on the fatigue and extreme loading of container vessels, 2014. International Journal of Naval Architecture and Ocean Engineering, 6(4), https://doi.org/https://doi.org/10.2478/IJNAOE-2013-0233

[2] Pal, S. K., Ono, T., Takami, T., Tatsumi, A., and Iijima, K., Effect of springing and whipping on exceedance probability of vertical bending moment of a ship, 2022. Ocean Engineering, 226. https://doi.org/10.1016/j.oceaneng.2022.112600

[3] Gan, J., Lin, X., Lin, H., Wang, Z., and Wu, W., Experimental study on the fatigue damage of designed T-type specimen with high-low frequency superimposed loading, 2021. *International Journal of Fatigue, 143*. 105985. https://doi.org/10.1016/j.ijfatigue.2022.107043

[4] Gan, J., Lin, X., Lin, H., Wang, Z., and Wu, W., Effect of high-low frequency superimposed loading on the fatigue crack propagation of longi-web connection joint. 2022. *International Journal of Fatigue, 163*. 107043 https://doi.org/10.1016/j.ijfatigue.2022.107043

[5] Gaspar, B., Teixeira, A., and Guedes Soares, C., Effect of the nonlinear vertical wave-induced bending moments on the ship hull girder reliability. 2016. *Ocean Engineering, 119*, 193-207. https://doi.org/10.1016/j.oceaneng.2015.12.005

[6] Storhaug, G., Experimental investigation of wave induced vibrations and their effect on the fatigue loading of ships, 2007. (Doctoral dissertation). Department of Marine Technology, Norwegian University of Science and Technology (NTNU), Oslo.

[7] Bouscasse, B., Merrien, A., Horel, B. and De Hauteclocque, G., 2022. Experimental analysis of wave-induced vertical bending moment in steep regular waves. *Journal of Fluids and Structures, 111*, 103547. https://doi.org/10.1016/j.jfluidstructs.2022.103547

[8] Waskito, K., T., Kashiwagi, M., Iwashita, H., Hinatsu, M., Prediction of nonlinear vertical bending moment using measured pressure distribution on ship hull, 2020. *Applied Ocean Research, 101*, 102261. https://doi.org/10.1016/j.apor.2020.102261

[9] Pferdekamper, K. and Bekker, A., Full-scale fatigue damage investigation of a slamming-prone vessel with unique section modulus characteristics, 2021. Conference: 8th International Conference on Marine Structures, Trondheim.

[10] Zhao, W., Leira, B. J., Feng, G., Gao, C., and Cui, T., A reliability approach to fatigue crack propagation analysis of ship structures in polar regions, 2021. *Marine Structures, 80*, 103075. https://doi.org/10.1016/j.marstruc.2021.103075

[11] DNV, Finite element analysis, 2021. (Det Norske Veritas). Class Guideline, DNV-CG-0127.

[12] DNV, Fatigue design of offshore steel structures, 2021. (Det Norske Veritas). Recommended Practice, DNV-RP-C203.

[13] Adland, R., Cariou, P., and Wolff, F. C., Optimal ship speed and the cubic law revisited: Empirical evidence from an oil tanker fleet, 2020. *Transportation Research Part E: Logistics and Transportation Review, 140*, 101972. https://doi.org/10.1016/j.tre.2020.101972

[14] Lakshmynarayanana, P. A., and Hudson, D., Estimating Added Power in Waves for Ships Through Analysis of Operational Data, 2017. *2nd Hull Performance and Insight Conference*, Germany.

[15] Guedes Soares, C. and Moan, T., 1991. Model uncertainty in the long-term distribution of wave-induced bending moments for fatigue design of ship structures. *Marine Structures, 4(4)*, 295-315. https://doi.org/10.1016/0951-8339(91)90008-Y

[16] IACS, 2012. Common structural rules for double hull oil tankers. International Association of Classification Societies, London.

[17] Newman, J., and Raju, I., An empirical stress-intensity factor equation for the surface crack, 1981. *Engineering Fracture Mechanics, 15(1)*, 185-192. https://doi.org/10.1016/0013-7944(81)90116-8

[18] British Standard, Guide to methods for assessing the acceptability of flaws in metallic structures, 2005. BS 7910:2005.

[19] ABS, Guide for fatigue assessment of offshore structures, 2020. American Bureau of Shipping (ABS), Texas, USA.